



Research paper

A new ANN rheological model of a comply polymer in temperature spectrum

Anna M. Stręk

Abstract: The article presents modelling using artificial neural networks (ANN) of the phenomenon of creep of comply polymer SIKA PS which can be used in various applications in civil engineering. Data for modelling was gathered in compressive experiments conveyed under a set of fixed conditions of compressive stress and temperature. Part of the data was pre-processed by smoothing and rediscritisation and served as inputs and targets for network training and part of the data was left raw as control set for verification of prognosing capability. Assumed neural network architectures were one- and two-layer feedforward networks with Bayesian regularisation as a learning method. Altogether 55 networks with 8 to 12 neurons in varying structural configurations were trained. Fitting and prognosing verification was performed using mean absolute relative error as a measure; also, results were plotted and assessed visually. In result, the research allowed for formulation of a new rheological model for comply polymer SIKA PS in time, stress and temperature field domain with fitting quality of mean absolute relative error 1.3% and prognosis quality of mean absolute relative error 8.73%. The model was formulated with the use of a two-layer network with 5 + 5 neurons.

Keywords: comply polymer, creep, neural networks, rheological model, temperature spectrum

1. Introduction

Comply polymers are materials widely used in civil engineering technology. Exemplary applications comprise: connections in structural elements [1], reinforcement of traditional building materials like bricks or timber [2], reinforcement of historic or heritage buildings or structures [3], bonding layers in protection composites against earthquake-induced pounding of buildings [4]. The given examples do not, of course, exhaust the field of application of comply polymers in the building industry and civil engineering; however, they show some characteristic conditions in which these materials can work. Namely, the discussed materials can be subjected to long-term loads (*e.g.* considerable self-weight of a structure) and exposure to elevated temperatures – *e.g.* direct solar radiation on a masonry of a historical *façade* in a hot climate or special structures exposed to thermal radiation.

It would be then favourable for the designers to have a good source of knowledge allowing for incorporation of long-term effects of loading like creep but also the impact of high temperature in polymers used in structural design. Additionally, knowledge of the rheological behaviour of polymers subjected to loading at elevated temperatures could also be used to improve fire protection of structures in which they would be used. Among a wide range of publications which address these problems, the following examples could be mentioned: [5–7]. Also, the research reported in the present article is devoted to description of the phenomenon of creep in temperature field.

Since the most convenient source for designers would be a rheological model in a mathematical form, which could be easily implemented to CAD software, the undertaken research aimed at derivation of such a model. For this purpose artificial neural networks (ANN) were used. Neural networks are a modern tool successfully used in various fields of civil engineering [8–10]. It can be applied to finding description of multi-parameter, nonlinear and complex phenomena – such as creep in temperature spectrum. Examples of neural network analysis for other nonlinear and parameter-related phenomena for materials which recently also find application in structural engineering include *e.g.* [11].

In the present research the modelling was performed for SIKA PS material, which is a type of a polyurethane. Calculations were conveyed using experimental data reported in [5]. The software used was Matlab R2017b and R2019A and auxiliarily MSOffice 2016 and GIMP. Training of a set of networks and evaluation of their results according to assumed error criteria allowed for finding a mathematical form of a rheological model of satisfactory accuracy.

2. Data for neural network modelling

Neural network calculations were performed basing on experimental data from research reported in [5]. The studied material was compliant polymer PS produced by SIKA. The experiments consisted in measurement of strain for cylindrical specimens subjected to constant compression for about 100 hours under constant temperature. Three values of compressive stress were assumed: 0.5, 1.0, 2.0} MPa. For each stress value creep was

measured in four temperature conditions: 20, 40, 60, 80°. Specimens' dimensions were: diameter $d = 27$ mm and height $h = 54$ mm. Results of experiments are depicted in Fig. 1.

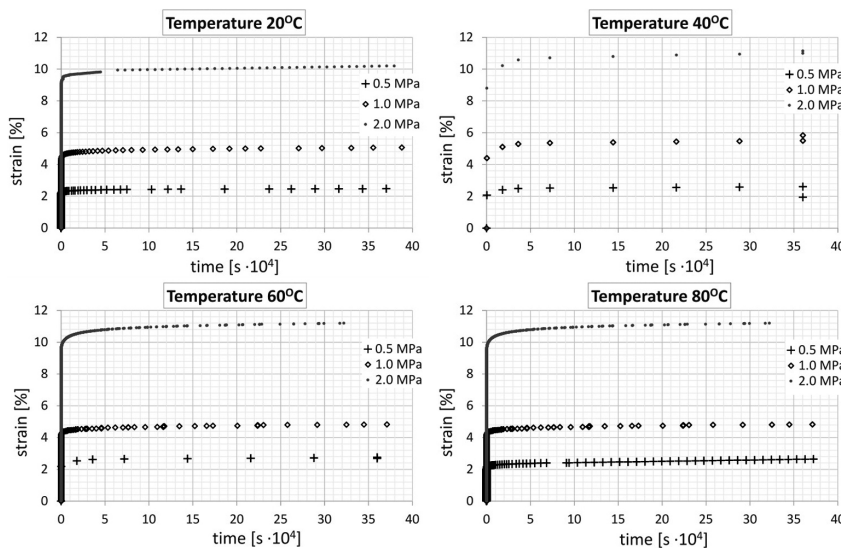


Fig. 1. Results of creep testing in temperature spectrum

Number of data gathered for the three specimens tested in 40° and for the specimen compressed with 0.5 MPa in 60° was considerably smaller than data gathered for other samples. Such disproportion could introduce undesired and possibly adverse bias in network training, so results for those 4 samples were excluded from modelling and later used as control data for evaluation of prognosing capability of networks. Data for the remaining 8 specimens were pre-processed to eliminate the potential bias due to non-uniform distribution over time domain, different vector lengths and local discontinuities which could have been derivative of load and displacement transducer signals. It consisted in smoothing and interpolation using cubic smoothing splines [14], in the domain of time and afterwards rediscretisation.

Inbuilt Matlab function *csaps* was used for cubic smoothing spline interpolation [16] with a smoothing parameter $p \in (0, 1)$ whose mathematical role is given in [16]. In the present study it was chosen from the allowed range by evaluation of the time-strain plots corresponding to the raw and smoothed data. It was assumed $p = 0.1$ for all specimens; apart from specimen PS_2_80 for which it was chosen $p = 0.6$ and specimens PS_2_20, PS_1_60 for which it was adopted $p = 0.0004$ (first numerical value in a sample's name refers to stress in MPa and the second to temperature in Celsius degrees). It was decided to introduce decreasing distribution of data in the time domain during rediscretisation, according to the fact that creep is a more dynamic process at the beginning. Time intervals for rediscretisation and used sampling frequencies are set in Table 1. After pre-processing, data points for all specimens had the same vector length equal to 304 and were distributed in the same way over the same time interval.

Table 1. Time intervals for rediscretisation and used sampling frequencies

Time domain interval	0÷60 s	60÷120 s	2÷20 min	10 min÷15 h	15÷100 h
Frequency of sampling	0.5 s	1 s	1 min	10 min	5 h

3. Neural network modelling

3.1. Assumptions for model form, inputs, targets and learning parameters

Experimental data shows that creep strain ε is a function of time t and two set parameters: compressive stress σ and temperature T . Thus, the modelled relation can be generalised to a hypersurface over a three-dimensional domain: $\varepsilon = f(\sigma T t)$. Hence, arguments for networks training were assumed as vectors $\text{input}_i = [\sigma \ T \ t]^T$, where entries' values exhausted all sequences of: $\sigma \in \{500, 1000, 2000\}$ kPa, $T \in \{20, 60, 80\}^\circ\text{C}$, $0 < t < 360000$ s with sampling form Table 1; $i \in \langle 1, 24, 32 \rangle$. Targets for the networks were assumed as scalars $\text{target}_i = \varepsilon$, being pre-processed experimental strains in [%] respective for given stress, temperature and time. Inputs and targets were normalised at entry to networks and denormalised on exit; inbuilt Matlab function *mapminmax* [17] was used for simplification of this process.

General architecture of networks was assumed as feedforward with one or two hidden layers. The hyperbolic tangent sigmoid function (*tansig*) [18] was adopted as the activation function in the hidden layer or layers. In the output layer the activation function was set as linear (*purelin*) [18]. The number of neurons in the hidden layer or layers was to be assessed in result of the presented research, while the number of neurons in the output layer was set as 1. As for the learning method, it was decided to use Bayesian regularisation backpropagation [19, 20] with two learning stages: training and testing. In Bayesian regularisation typically there is no validation stage separated, because its algorithm minimises not solely squared errors but the combination of squared errors and squared weights [19–21]. If validation failure threshold would be introduced, then it could stop training for large weights even if error would be converging to zero [21]. Data attribution to network learning stages was assumed as: 85% to training and 15% to test. The number of epochs, learning gradient and momentum were calibrated separately for networks with one or two hidden layers.

Fitting capability of trained networks was evaluated using mean relative absolute error (*MARE*) from learning. Prognosing capability was verified using mean relative absolute error (*MARE^P*) for control data. However, because the control set was sparse, qualitative verification was also performed. This evaluation was approached by examination of plots of networks' prognosis in an increased domain: compressive stress parameters were assumed as $\sigma = \langle 400, 2100 \rangle$ kPa with interval 100 kPa. Time and temperature domains were not changed. Visual approach was justified, because the phenomenon is ordered.

3.2. One hidden layer networks

Initially, 10 neurons were designed for the hidden layer in the one-layer network type. Three sets of varying hyperparameters were assumed for calibration, they are shown in Table 2. For each HPset five 10-neuron networks (named: *instances*) were trained and tested. Mean absolute relative errors were calculated for each instance and they are depicted in the left plot in Fig. 2 as diamonds. One can see that HPset 1.1 led to larger *MARE* values, so it was rejected. HPset 1.2 generated slightly better results than HPset 1.3, so it was chosen. On the whole, 10-neuron networks with sets 1.2 and 1.3 resulted in very good fitting, as they reached $MARE \leq 6\%$. The best result was reached for 10-neuron network HPset 1.2 instance 5: $MARE_{10_HP1.2_5} = 4.98\%$.

Table 2. Hyperparameter sets used for their calibration in one-layer networks

Hyperparameters set	Number of epochs	Learning gradient	Momentum
HPset 1.1	3000	$1e^{-10}$	0.1
HPset 1.2	10000	$1e^{-10}$	0.1
HPset 1.3	10000	$1e^{-15}$	0.0001

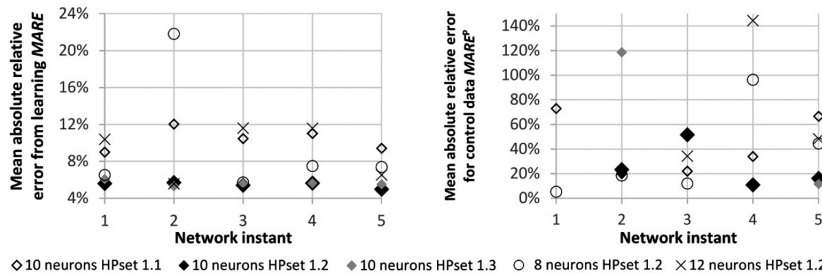


Fig. 2. Mean absolute relative error for fitting (left) and prognosis (right) of one-layer networks

In attempt to finding a simpler model, 5 instances of networks with 8 neurons with the chosen HPset 1.2 were trained. Results of mean absolute relative error are shown in the left plot in Fig. 2 as circles. One observes that lowering the number of neurons by 2 caused some decrease of fitting quality. For comparison also 5 instances of networks with 12 neurons and HPset 1.2 were trained. The results of *MARE* for them are depicted in the left plot in Fig. 2 as x-es, one sees that on average they also had worse fitting capability than 10-neuron networks.

The right plot in Fig. 2 gives mean absolute relative errors calculated for verification of prognosing capability of networks performed on control data. Six instances (4 with 10 neurons and 2 with 12) resulted in $MARE^P > 1300\%$ and are not depicted in the graph. This fact shows that for networks with more than 8 neurons considerable overfitting tends to occur. On the other hand, the best result was obtained for 8-neuron network HPset 1.2 instance 1: $MARE_{8_HP1.2_1}^P = 5.36\%$. The respective $MARE_{8_HP1.2_1} = 6.52\%$ expressing

fitting quality of this network was also on a satisfactory level. Figure 3 presents results of verification on control data (left) and with respect to increased stress domain (right, only outputs for $T = 60^\circ$ are depicted for clarity). The graphs prove that the 8-neuron model is quite good; however, monotonicity in the stress domain is disturbed around the middle of the field and the model does not prognose the initial arch curvature distinctly at the beginning of the time range.

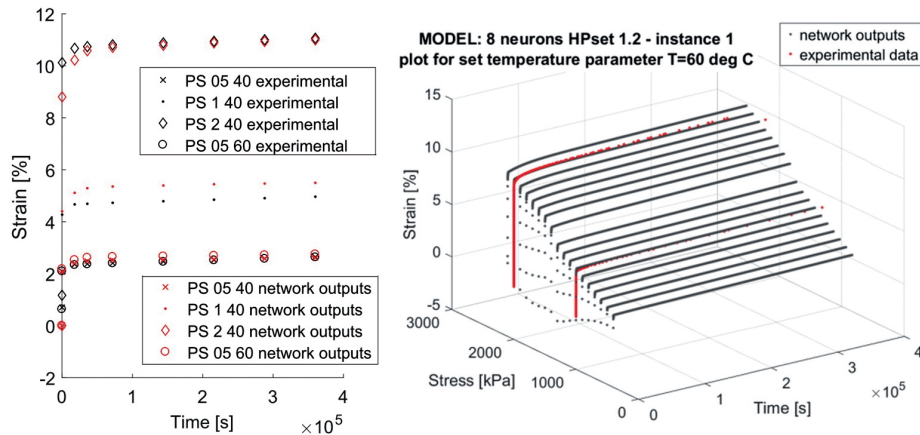


Fig. 3. The best one-layer model verification on control data (left) and increased stress domain (right)

The network with the second best verification $MARE_{10_HP1.2_4}^P = 10.96\%$ had the same flaws at visual check but to a slightly higher extent. The third best mean absolute relative error on control data was $MARE_{10_HP1.3_5}^P = 11.72\%$ and even though this value did not indicate much overfitting, its visual verification proved that the network also had to be rejected (Fig. 4).

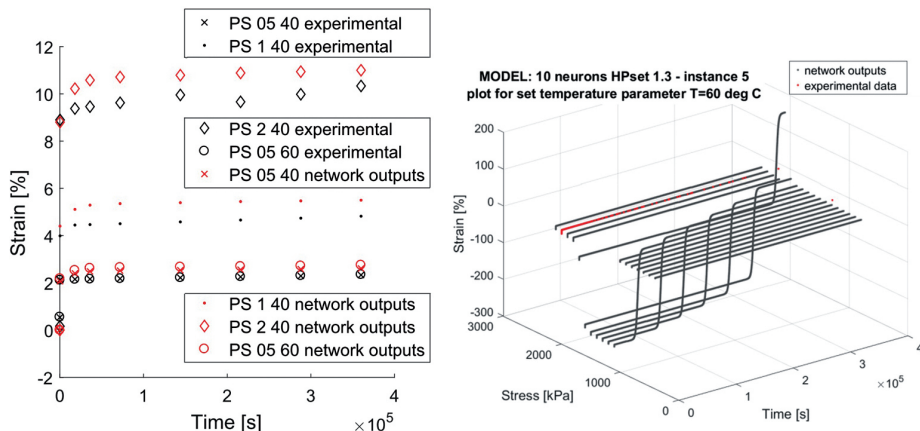


Fig. 4. An example of overfitted one-layer model: verification on control data (left) and increased stress domain (right)

3.3. Two hidden layers networks

In attempt to overcome the problems with the initial curvature and monotonicity in the stress domain, two-layer networks, starting from 6 + 6 neurons, were implemented. Again, 3 sets of hyperparameters were assumed (Table 3) and calibrated by comparison of 5 instances of trained networks for each set of them. Results of $MARE$ for them are shown in the left plot in Fig. 5 as diamonds. HPset 2.1 generated the highest $MARE$ for three instances, so it was rejected. From the remaining two sets, HPset 2.3 was slightly better, so it was chosen. Both HPsets 2.2 and 2.3 allowed for very good fitting with $MARE$ not exceeding 3.6%. In the next step, decreasing the complexity of models down to 5 + 5 neurons (10 instances) and 4 + 4 neurons (5 instances) was performed. Results of fitting assessment showed that both architectures are only slightly worse in fitting than the 6 + 6 one and except for one instance they fulfil $MARE \leq 6.7\%$ (Fig. 5, left).

Table 3. Hyperparameter sets used for their calibration in two-layer networks

Hyperparameters set	Number of epochs	Learning gradient	Momentum
HPset 2.1	3000	$1e^{-10}$	0.1
HPset 2.2	3000	$1e^{-15}$	0.0001
HPset 2.3	10000	$1e^{-15}$	0.0001

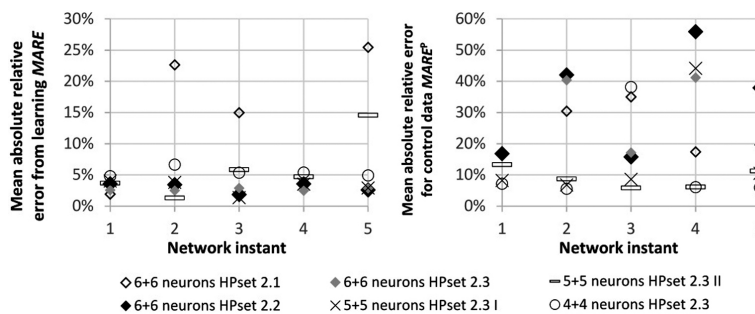


Fig. 5. Mean absolute relative error for fitting (left) and prognosis (right) of two-layer networks

The right plot in Fig. 5 presents results of verification of prognosing capability of networks performed on control data. Two instances of 6 + 6 networks had $MARE^P > 300\%$ and are not shown in the plot. On the average, good results – $MARE^P < 10\%$ – were obtained for most 5 + 5 and 4 + 4 networks. The second instance of the 4 + 4 architecture achieved the lowest error $MARE_{4+4_HP2.3_2}^P = 5.55\%$. For this network also fitting was satisfactory $MARE_{4+4_HP2.3_2} = 6.65\%$, even though not the best. These results are only slightly worse than for the best one-layer network, but the visual verification disqualifies this model – Fig. 6. The sparse character of the control data was very misleading in case of two-layer networks. Not until the 10th best result of $MARE^P$ did the visual evaluation confirm prognosis capability of the given network. It was the network with 5 + 5 neurons

in instance 7 and it will be described in detail in the next section, since – due to its good quality – it was assumed as the sought rheological model.

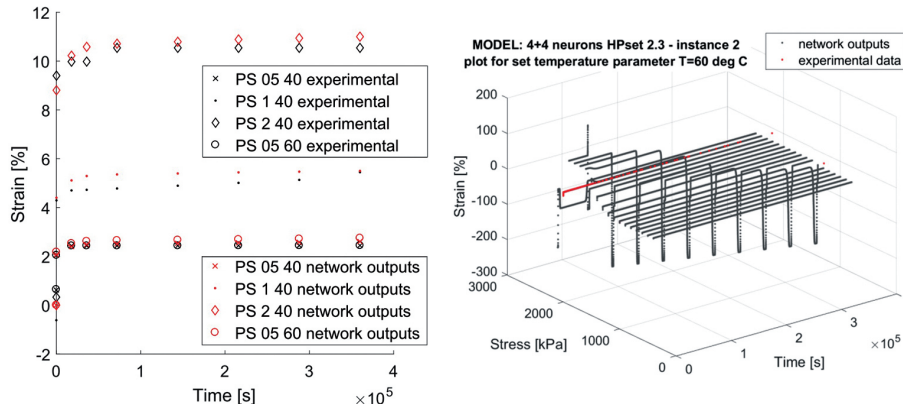


Fig. 6. Model 4 + 4_HP2.3_2 verified on control data (left) and increased stress domain (right)

4. Assumed rheological model and conclusions

The network with 5 + 5 neurons trained in instance 7 achieved the best fitting quality of all networks: $MARE_{5+5_HP2.3_7} = 1.30\%$. Histogram of all relative errors from learning is given in Fig. 7, left. The prognosis quality was satisfactory: $MARE_{5+5_HP2.3_7}^P = 8.73\%$. All relative errors from verification of the network on external data is shown in Fig. 7, right.

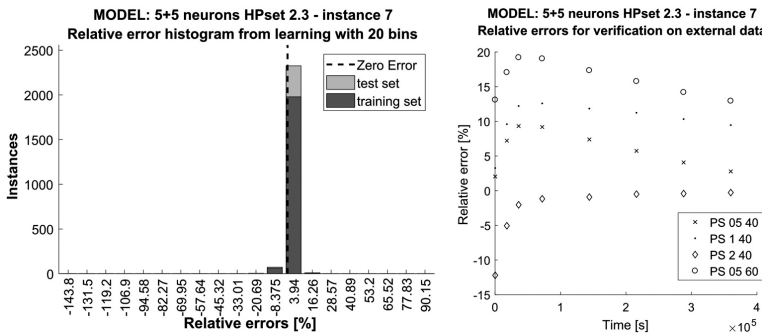


Fig. 7. Histogram of relative errors for learning (left); relative errors for external verification (right)

Figure 8 presents results of verification of this network. There can be observed slight imperfections of prognosis, like: the network sometimes miscalculates strain for first seconds (up to maximally 100 s), especially for $T = 20^\circ$. Also in case of $\sigma \geq 1.6$ MPa some small disturbance after the first plot curvature may be noticed at $T = 80^\circ$. These flaws; however, are not significant enough to disqualify the network.

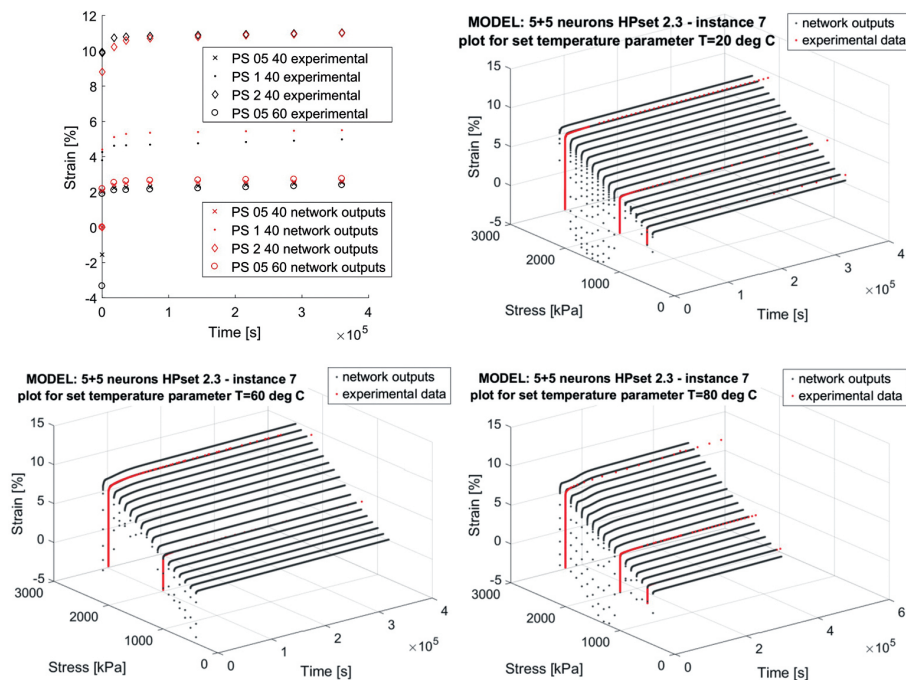


Fig. 8. Verification of the chosen model on control data (top left) and increased stress domain (other)

The mathematical form of the modelled rheological relation valid in domain ranges $\sigma \in \langle 500, 2000 \rangle$ kPa, $T \in \langle 20, 80 \rangle^\circ$ and $t \in \langle 0, 360\,000 \rangle$ s has the following form:

$$(4.1) \quad \varepsilon = \text{mapminmax}^{-1}$$

$$\left(\mathbf{W}_3 \cdot \left[\tanh_V \left(\mathbf{W}_2 \cdot \left[\tanh_V \left(\mathbf{W}_1 \cdot \text{mapminmax} \left([\sigma \ T \ t]^T \right) \right) + \mathbf{b}_1 \right] + \mathbf{b}_2 \right) \right] + \mathbf{b}_3 \right)$$

where:

$$\tanh_V \left([V_1 \ V_2 \ \dots \ V_n]^T \right) = [\tanh(V_1) \ \tanh(V_2) \ \dots \ \tanh(V_n)]^T$$

$$\mathbf{W}_1 = \begin{bmatrix} -6.3043 & -9.8479 & 0.1380 \\ 1.3740 & 1.7362 & -7.5790 \\ 1.3311 & 1.6333 & 29.6612 \\ 0.0233 & 0.0053 & -78.0055 \\ -0.3035 & 0.0198 & -0.0146 \end{bmatrix}$$

$$\mathbf{W}_2 = \begin{bmatrix} -0.2142 & -95.3983 & 97.0597 & -66.7866 & 22.9747 \\ 0.7101 & 63.2123 & -64.1407 & 136.9702 & 26.4466 \\ -0.2685 & -91.7926 & 93.3548 & -69.7182 & 19.4908 \\ 0.0309 & 0.0150 & -0.0016 & 0.0346 & 6.7901 \\ -1.0930 & -76.0821 & 77.0889 & -204.9043 & -48.5940 \end{bmatrix}$$

$$\mathbf{W}_3 = [13.8146 \ -1.1269 \ -13.4513 \ -31.0290 \ -0.3778]$$

$$\mathbf{b}_1 = [2.1879 \ -8.7804 \ 28.5335 \ -78.0819 \ -1.6468]^T$$

$$\mathbf{b}_2 = [16.5385 \ 36.1464 \ 12.9678 \ 8.2673 \ -63.1653]^T$$

$$b_3 = 28.7370$$

mapminmax – inbuilt Matlab functions for normalisation and denormalisation, equivalent to:

$$(4.2) \quad V' = \frac{V - V_{\min}}{V_{\max} - V_{\min}} \cdot (V'_{\max} - V'_{\min}) + V'_{\min}$$

where: V' – the new value; V – the original value; V_{\max}, V_{\min} – original interval limits; V'_{\max}, V'_{\min} – new limits, here: -1 and 1; for output denormalisation to strain: $V_{\varepsilon,\max} = 11.2420\%$, $V_{\varepsilon,\min} = 0$.

The presented research showed that the phenomenon of creep in spectrum of temperatures and for various compressive stress can be successfully modelled using neural networks. Complexity of the model is medium, since it requires deep learning with 5 + 5 neurons. The model achieves very good fitting quality with mean absolute relative error 1.3% and satisfactory prognosis quality with mean absolute relative error 8.73%. Further study would comprise broader calibration of hyperparameters, which might lead to more effective training performance. Also, training of more instances of the same or similar network architectures could result in improving prognosis quality.

Acknowledgements

I would like to express my special gratitude to Prof. B. Zajac for sharing experimental results and also to Prof. T. Machniewicz and Dr. M. Dudzik for fruitful advice and conversation.

References

- [1] J. Pečník, et al., "Mechanical performance of timber connections made of thick flexible polyurethane adhesives", *Engineering Structures*, vol. 247, no. 13, 2021, DOI: [10.1016/j.engstruct.2021.113125](https://doi.org/10.1016/j.engstruct.2021.113125).
- [2] A. Kwiecień, P. Krajewski, Ł. Hojdys, M. Tekieli, and M. Słonński, "Flexible Adhesive in Composite-to-Brick Strengthening – Experimental and Numerical Study", *Polymers*, vol. 10, no. 4, art. no. 356, 2018, DOI: [10.3390/polym10040356](https://doi.org/10.3390/polym10040356).
- [3] A. Kwiecień, K. Rodacki, B. Zajac, and T. Kozik, "Mechanical Behavior of Polyurethane Adhesives Applied to Timber Joints in Repair of Historical Timber Structures: An Interdisciplinary Approach" in *RILEM Bookseries, vol. 18: Structural Analysis of Historical Constructions*, R. Aguilar, et al., Eds. Springer, 2019, pp. 1603–1612, DOI: [10.1007/978-3-319-99441-3_172](https://doi.org/10.1007/978-3-319-99441-3_172).
- [4] A. M. Stręk, et al., "Highly Dissipative Materials for Damage Protection against Earthquake-Induced Structural Pounding", *Materials*, 2021, vol. 14, no. 3231, 2021, DOI: [10.3390/ma14123231](https://doi.org/10.3390/ma14123231).
- [5] B. Zajac, *Ścinane połączenia klejone sztywne i podatne pracujące w podwyższonej temperaturze*. Kraków: Wydawnictwo PK, 2018.
- [6] Z. Bogusław and K. Arkadiusz, "Thermal Compatibility of Rigid and Flexible Adhesives to Substrates of Historical Structures", in *RILEM Bookseries, vol. 18: Structural Analysis of Historical Constructions*, R. Aguilar, et al., Eds. Springer, 2019, pp. 1868–1877, DOI: [10.1007/978-3-319-99441-3_200](https://doi.org/10.1007/978-3-319-99441-3_200).

- [7] Z. Bogusław, K. Arkadiusz, M. Gams, and T. Tatara, “Strengthening of masonry and concrete structures working in elevated temperatures and mining tremors area”, *E3S Web of Conferences*, 2019, vol. 106, pp. 1–8, DOI: [10.1051/e3sconf/201910601021](https://doi.org/10.1051/e3sconf/201910601021).
- [8] Z. Waszczyzyn and L. Ziemiński, “Neural networks in the identification analysis of structural mechanics problems”, in *Parameter identification of materials and structures*, Z. Mróz, G. E. Stavroulakis, Eds. Springer, 2005, pp. 265–340, DOI: [10.1007/3-211-38134-1_7](https://doi.org/10.1007/3-211-38134-1_7).
- [9] I. Floodm and N. Kartam, “Neural network in civil engineering I: Principles and understandings”, *ASCE Journal of Computing in Civil Engineering*, vol. 8, no. 2, pp. 131–148, 1994, DOI: [10.1061/\(ASCE\)0887-3801\(1994\)8:2\(131\)](https://doi.org/10.1061/(ASCE)0887-3801(1994)8:2(131)).
- [10] I. Flood and N. Kartam, “Neural network in civil engineering II: Systems and application”, *ASCE Journal of Computing in Civil Engineering*, vol. 8, pp. 149–162, 1994, DOI: [10.1061/\(ASCE\)0887-3801\(1994\)8:2\(149\)](https://doi.org/10.1061/(ASCE)0887-3801(1994)8:2(149)).
- [11] M. Dudzik, A. M. Stręk, “ANN model of stress-strain relationship for aluminium sponge in uniaxial compression”, *Journal of Theoretical and Applied Mechanics*, vol. 58, no. 2, pp. 385–390, 2020, DOI: [10.1563/jtampl/116804](https://doi.org/10.1563/jtampl/116804).
- [12] A. M. Stręk, M. Dudzik, and T. Machniewicz, “Specifications for modelling of the phenomenon of compression of closed-cell aluminium foams with neural networks”, *Materials*, 2022, vol. 15, no. 3, 2022, DOI: [10.3390/ma15031262](https://doi.org/10.3390/ma15031262).
- [13] M. Dudzik and A. M. Stręk, “ANN architecture specifications for modelling of open-cell aluminum under compression”, *Mathematical Problems in Engineering*, vol. 2020, art. no. 834317, pp. 1–26, 2020, DOI: [10.1155/2020/2834317](https://doi.org/10.1155/2020/2834317).
- [14] C. H. Reinsch, “Smoothing by spline functions”, *Numerische Mathematik*, vol. 10, pp. 177–184, 1967, DOI: [10.1007/BF02162161](https://doi.org/10.1007/BF02162161).
- [15] R. Champion, C. T. Lenard, and T. M. Mills, “An introduction to abstract splines”, *Mathematical Sciences*, vol. 21, pp. 8–26, 1996.
- [16] Mathworks documentation, “Csaps”. [Online]. Available: www.mathworks.com/help/curvefit/csaps.html. [Accessed: 21 Nov. 2021].
- [17] Mathworks documentation: “Mapminmax”. [Online]. Available: www.mathworks.com/help/deeplearning/ref/mapminmax.html. [Accessed: 21 Feb 2019].
- [18] H. Demuth, M. Beale, and M. T. Hagan, *Neural Network Toolbox 6 User’s Guide*. The MathWorks Inc., 2009.
- [19] F. D. Foresee and M. T. Hagan, “Gauss-Newton approximation to Bayesian learning”, *Proceedings of the International Joint Conference on Neural Networks (ICNN’97)*, vol. 3, pp. 1930–1935, 1997, DOI: [10.1109/ICNN.1997.614194](https://doi.org/10.1109/ICNN.1997.614194).
- [20] D. J. C. MacKay, “Bayesian interpolation”, *Neural Computation*, vol. 4, no. 3, pp. 415–447, 1992, DOI: [10.1162/neco.1992.4.3.415](https://doi.org/10.1162/neco.1992.4.3.415).
- [21] Mathworks MATLAB Answers, “Why does the “trainbr” function not require a validation dataset?”. [Online]. Available: <https://www.mathworks.com/matlabcentral/answers/405727-why-does-the-trainbr-function-not-require-a-validation-dataset>. [Accessed: 28 Apr. 2022].

Nowy model reologiczny dla polimeru podatnego w spektrum temperatur uzyskany za pomocą sztucznych sieci neuronowych

Słowa kluczowe: model reologiczny, pełzanie, polimer podatny, sieci neuronowe, spektrum temperatur

Streszczenie:

Polimery podatne stanowią ważny materiał wykorzystywany w budownictwie oraz inżynierii lądowej. Ich zastosowania obejmują często połączenia klejone elementów konstrukcyjnych, mogą być

wykorzystane do wzmacniania zabytkowych konstrukcji murowych w miejscu uszkodzonej zaprawy, a także jako warstwy łączące w zabezpieczeniach przeciwzderzeniowych budynków przy zagrożeniu trzęsieniami ziemi, jak również jako składniki dylatacyjne. Podane przykłady nie wyczerpują oczywiście zakresu stosowalności rozważanego materiału w budownictwie, pokazując jednak, że w czasie pracy może być on poddany długotrwały stały obciążeniom (np. ciężar własny) oraz ekspozycji na podwyższone temperatury – np. bezpośrednie promieniowanie słoneczne na murowaną zabytkową elewację w gorącym klimacie lub obiekty specjalne, w których jest radiacja cieplna. Znajomość zachowania materiału poddanego obciążeniu długotrwałemu w podwyższonej temperaturze może być wykorzystana także do polepszenia ochrony pożarowej budowli.

W artykule zaprezentowano badania służące opracowaniu modelu reologicznego dla polimeru podatnego PS Sika oraz nową propozycję takiego modelu. Zastosowano obliczenia z wykorzystaniem sztucznych sieci neuronowych, dla których dane uczące oraz dane kontrolne stanowiły wyniki eksperymentalne. Eksperymenty polegały na ściskaniu próbek walcowych o średnicy $d = 27$ mm i wysokości $h = 54$ mm. Czas obciążania wynosił około 100 h, zastosowano warunki stałe temperatury $\{20, 40, 60, 80\}^\circ$ oraz stałe warunki naprężenia $\{0.5, 1.0, 2.0\}$ MPa w 12 kombinacjach.

Do modelowania neuronowego wykorzystano sieci jedno- i dwuwarstwowe z nauczycielem. Przyjęto uczenie metodą propagacji wstecznej – regularizacji Bayesa. Jako funkcję celu wybrano średni błąd kwadratowy i jego wartość docelową równą zero. W warstwach ukrytych jako funkcję aktywacji zastosowano tangens sigmoidalny, natomiast w warstwie wyjścia przyjęto jako funkcję aktywacji funkcję liniową. Hiperparametry, takie jak moment, gradient i liczba epok zostały skalibrowane osobno dla sieci jedno- i dwuwarstwowych. Jakość dopasowania sieci do danych z uczenia była mierzona za pomocą średniej z wartości bezwzględnych z błędów względnych pomiędzy wynikiem z sieci i odpowiednią wartością danej przeznaczonej do uczenia (oznaczono jako $MARE$). Z kolei jakość zdolności sieci do uogólniania (przewidywania poza znany zakresem) była mierzona za pomocą średniej z wartości bezwzględnych z błędów względnych pomiędzy wynikiem z sieci i odpowiednią wartością danej kontrolnej, oznaczono jako $MARE^P$. Oprócz tego jakość prognozowania weryfikowano za pomocą wykresów kontrolnych wyników z sieci obliczanych przy poszerzonym zakresie dziedziny naprężzeń.

Modelowanie neuronowe rozpoczęto od struktur jednowarstwowych z 10 neuronami w warstwie ukrytej i trzech różnych zestawów hiperparametrów, dla każdego zestawu uczonego 5 sieci. Dzięki porównaniu otrzymanych wyników $MARE$ wybrano najlepszy zestaw parametrów uczenia. W kolejnym kroku uczonego po pięć sieci z 8 i 12 neuronami. Łącznie uczonego 25 sieci jednowarstwowych. Uzyskane modele wykazywały w ogólności dobrą jakość dopasowania do danych uczących, natomiast zdolności uogólniania były zróżnicowane i oprócz porównania $MARE^P$ konieczne było także porównanie wyników graficznych. Ostatecznie najlepszy model jednowarstwowy uzyskano z sieci o 8 neuronach, dla której parametry liczbowe oceny wynosiły $MARE^P = 5.36\%$ i $MARE = 6.52\%$, natomiast wyniki graficzne ujawniły niewielkie zaburzenia przy odwzorowaniu charakteru monotoniczności oraz krzywizny początkowego zakresu wykresów.

Podjęto próbę rozwiązania problemów z dokładnością odwzorowania za pomocą zwiększenia złożoności sieci – podejście to polegało na zaimplementowaniu sieci dwuwarstwowych. Rozpoczęto od struktur 6 + 6 neuronów, dla których przyjęto trzy zestawy hiperparametrów i wykonano po pięć przypadków uczenia dla każdego zestawu. Po porównaniu średnich z wartości bezwzględnych z błędów względnych tych 15 sieci, wybrano najlepszy zestaw i dla niego wytrenowano kolejne 15 sieci o zmniejszonej liczbie neuronów: dziesięć przypadków po 5 + 5 neuronów i pięć przypadków o strukturze 4 + 4 neurony. Ostatecznie, na podstawie ilościowej oceny dopasowania i zdolności prognozowania sieci, a także dokonując porównania wyników w formie graficznej, uzyskano sieć, którą wybrano jako model reologiczny zachowania się polimeru PS w zakresie stałych naprężień

oraz temperatur w dziedzinie czasu: $\sigma \in \langle 500, 2000 \rangle$ kPa, $T \in \langle 20, 80 \rangle^\circ$ oraz $t \in \langle 0, 360\,000 \rangle$ s. Równanie modelu pokazano w artykule. Miary jakości dla modelu wynosiły odpowiednio: $MARE = 1.30\%$ i $MARE^P = 8.73\%$.

Modelowanie neuronowe opisane w artykule pozwoliły na ujęcie formalne skomplikowanego zjawiska pełzania w zależności od parametrów naprężenia i temperatury. Dzięki zastosowaniu dwóch warstw udało się poprawić modelowanie początku krzywizny oraz charakteru monotoniczności wykresów w porównaniu do przypadku jednowarstwowego. W ramach kontynuacji badań, planowane jest poszukiwanie modelu o jeszcze lepszej zdolności uogólniania ($MARE^P < 5\%$) i z polepszonym odwzorowaniem początków zakresu dziedziny czasu. Badania te mogłyby zostać zrealizowane poprzez poszerzenie zakresu doboru hiperparametrów przy uczeniu, modyfikację struktur sieci, większą liczbę powtórzeń uczenia dla danej architektury.

Received: 2022-06-27, Revised: 2022-07-12